Inorg. Chem. **2004**, *43*, 3976–3987

Stereoelectronic Influence of the Type of Bifunctional *ansa*-Monocyclopentadienyldimethylsilylamido Ligand on the Molecular Structures Displayed by Zirconium Dichloride and 1,4-Diphenylbutadiene Complexes

Leonie F. Braun,[1] Thorsten Dreier,[1] Matthew Christy, and Jeffrey L. Petersen*

C. Eugene Bennett Department of Chemistry, West Virginia University, Morgantown, West Virginia 26505-6045

Received January 5, 2004

A series of organozirconium dichloride and 1,4-diphenylbutadiene complexes featuring a dianionic bifunctional ligand with a cyclopentadienyl-type functionality and an appended amido N donor have been prepared and structurally characterized. $[(C_5H_4)SiMe_2(N\text{-}t\text{-}Bu)]ZrCl_2$, **1**, $[(C_9H_6)SiMe_2(N\text{-}t\text{-}Bu)]ZrCl_2$, **2**, and $[(C_5Me_4)SiMe_2(N\text{-}i\text{-}Pr)]ZrCl_2$, **3**, were prepared in two steps, with ligand chelation accomplished by an amine elimination reaction followed by treatment of the diamido Zr intermediate with an excess of $SiMe_3Cl$. X-ray structural analyses reveal that in the solid state **2** is monomeric, whereas **1** and **3** are centrosymmetric dimers linked by a pair of bridging chlorides. The level of asymmetry displayed by the central $Zr_2(\mu\text{-}Cl)_2$ moiety is indicated by the variation in the pair of independent bridging Zr–Cl bond distances, which are 2.618(1) and 2.657(1) Å in **1** and 2.542(1) and 2.745(1) Å in **3**, respectively. The metathetical reactions of $[Mg(C_4H_4Ph_2)(THF)_3]_n$ with **1**, **2**, **3**, and $[(C_5Me_4)SiMe_2(N\text{-}t\text{-}Bu)]ZrCl_2$ proceed to afford the corresponding 1,4-diphenylbutadiene derivatives **4**, **5**, **6**, and **7**, respectively. Solution NMR data show that **6** is obtained exclusively as the supine isomer, whereas compounds **4**, **5**, and **7** exist as >20:1, 6:1, and 2:1 mixtures of the supine and prone isomers at ambient temperature. The molecular structures of the supine forms of **4**, **5**, **6**, and **7** are appreciably folded (70–80°) along the line of intersection between the plane containing the Zr and the two terminal butadiene carbons and the plane of the *cis*-butadiene fragment. An increase in the folding is accompanied by a decrease in the difference between the average Zr–C(terminal) and Zr–C(internal) bond distances and leads to a more pronounced long–short–long C–C bond sequence within the coordinated butadiene.

Introduction

The Lewis acidity of early-transition-metal metallocenes is enhanced by the replacement of the two cyclopentadienyl rings with a bifunctional *ansa*-cyclopentadienylamido ligand, such as $[(C_5Me_4)SiMe_2(N\text{-}t\text{-}Bu)]^{2-}$, which reduces the steric congestion and the formal electron count at the electrophilic center. This ligand modification was originally introduced by Bercaw and co-workers[2] and led to their development of one-component scandium-based ethylene polymerization catalysts. Researchers at The Dow Chemical Co.[3] and Exxon[4] extended Bercaw's findings to Group 4 metals and independently prepared a series of 14-electron *ansa*-cyclopentadienylamido metal complexes, $[(C_5R_4)L(NR')]MCl_2$, with M = Ti, Zr, Hf; R = H, alkyl; R′ = alkyl, aryl, which, upon activation with methylalumoxane, afford highly active Ziegler−Natta catalysts for the copolymerization of ethylene and 1-alkenes or styrene. The catalytic performance of these "constrained-geometry" catalysts varies with the electronic and steric features of the cyclopentadienyl and amido functionalities and the type of bridging linkage (L).[3−5]

The incorporation of an *ansa*-cyclopentadienylamido-type ligand is typically accomplished by a conventional metathesis

* Author to whom correspondence should be addressed. E-mail: jpeterse@wvu.edu.

(1) Institut für Organische Chemie, University of Münster, visiting student.

(2) (a) Shapiro, P. J.; Cotter, W. D.; Schaefer, W. P.; Labinger, J. A.; Bercaw, J. E. *J. Am. Chem. Soc.* **1994**, *116*, 4623−4640. (b) Piers, W. E.; Shapiro, P. J.; Bunel, E. E.; Bercaw, J. E. *Synlett* **1990**, *2*, 74−84. (c) Shapiro, P. J.; Bunel, E. E.; Schaefer, W. P.; Bercaw, J. E. *Organometallics* **1990**, *9*, 867−869.

(3) Stevens, J. C.; Timmers, F. J.; Rosen, G. W.; Knight, G. W.; Lai, S. Y. Eur. Patent Appl. EP 0 416 815 A2, 1991.

(4) Canich, J. M. Eur. Patent Appl. EP 0 420 436 A1, 1991.

(5) McKnight, A. L.; Masood, M. A.; Waymouth, R. M.; Straus, D. A. *Organometallics* **1997**, *16*, 2879−2885.

10.1021/ic040001i CCC: $27.50
Published on Web 05/27/2004

reaction of a suitable dilithio salt, a diGrignard reagent of $[(C_5R_4)L(NR')]^{2-}$ with an appropriate metal chloride,[2−7] or by a thermally induced amine elimination reaction of $(C_5R_4H)L(NHR')$ and a metal tetraamide.[8−11] The conversion of the intermediate metal diamido complex to the corresponding dichloride derivative may be accomplished by the addition of excess $SiMe_3Cl$. This latter approach has led to the development of efficient syntheses for $[(C_5H_4)SiMe_2(N\text{-}t\text{-}Bu)]TiCl_2$[10] and $[(C_5Me_4)SiMe_2(N\text{-}t\text{-}Bu)]ZrCl_2$[12] and was used to prepare the *ansa*-monocyclopentadienyldimethylsilylamido Zr dichloride complexes reported herein. Leung and co-workers[11] reported that treatment of enantiomerically pure *R*(−)- or *S*(+)-$[(C_5Me_4)SiMe_2(NCH(Me)Ph)]Zr(NMe_2)_2$ with $SiMe_3Cl$ initially led to the isolation of the *RR*- and *SS*-dichloro-bridged dimers, respectively, which upon sublimation (10^{-2} Torr, 200 °C) yield the respective monomeric *R*- and *S*-$[(C_5Me_4)SiMe_2(NCH(Me)Ph)]ZrCl_2$ complexes. Teuben and co-workers subsequently found that the modified amine elimination reaction of $Zr(NMe_2)_2Cl_2(THF)_2$[13] with $(C_5H_5)(CH_2)_nNHR$, $n = 2$, 3, affords $[(C_5H_4)(CH_2)_n(NR)]ZrCl_2$, R = *i*-Pr, *t*-Bu, directly in one step.[14]

The $[(C_5Me_4)SiMe_2(NR)]TiCl_2$ complexes are highly attractive precursors for the generation of olefin copolymerization catalysts.[15] Treatment of $[(C_5Me_4)SiMe_2(NR^1)]TiCl_2$ with 2 equiv of *n*-BuLi in the presence of excess diene allowed researchers at The Dow Chemical Co. in collaboration with Marks and co-workers[15a] at Northwestern University to prepare a series of organotitanium diene complexes, $[(C_5Me_4)SiMe_2(NR^1)]Ti(R^2CH{=}CHCH{=}CHR^3)]$ (R^1 = *t*-Bu, Ph; R^2 = H, Me; R^3 = H, Me). The stoichiometric addition of $B(C_6F_5)_3$ converts these Ti−diene complexes into zwitterionic complexes $[(C_5Me_4)SiMe_2(NR^1)]Ti^+R^2CH{=}CHCH{=}CHR^3B^-(C_6F_5)_3$, which function as single-component copolymerization catalysts. Cowley and co-workers[16] used a similar approach to prepare $[(C_5Me_4)SiMe_2(N\text{-}t\text{-}Bu)]M^+CHMe{=}CHCH{=}CH_2B^-(C_6F_5)_3$, M = Ti, Zr, and observed that the π-allyl unit within the cisoid butadiene adopts the *Z* configuration. Related Ti and Zr 1,3-butadiene complexes may also be prepared by the corresponding metathetical reactions of $[(C_5Me_4)SiMe_2(NR)]MCl_2$, R = *t*-Bu,[17] $CHMe(1\text{-}C_{10}H_7)$,[17] or $[(C_5H_4)SiMe_2(N\text{-}t\text{-}Bu)]MCl_2$,[18] with $[Mg(C_4H_6)(THF)_2]_n$.

The X-ray structural analyses of $[(C_5Me_4)SiMe_2(N\text{-}t\text{-}Bu)]Zr(C_4H_6)$[17] and $[(C_5H_4)SiMe_2(N\text{-}t\text{-}Bu)]Zr(C_4H_6)$[18] revealed that the replacement of C_5Me_4 with the C_5H_4 ring has a dramatic influence on the solution and solid-state structures displayed by these compounds. Solution NMR data for $[(C_5Me_4)SiMe_2(N\text{-}t\text{-}Bu)]Zr(C_4H_6)$ indicate the presence of an 85:15 mixture of the supine and prone isomers, whereas for $[(C_5H_4)SiMe_2(N\text{-}t\text{-}Bu)]Zr(C_4H_6)$, only the supine isomer is observed. In the solid state, the supine isomer of $[(C_5Me_4)SiMe_2(N\text{-}t\text{-}Bu)]Zr(C_4H_6)$ is mononuclear.[17] Alternatively, $[(C_5H_4)SiMe_2(N\text{-}t\text{-}Bu)]Zr(C_4H_6)$ is tetranuclear,[18] with four unsymmetrically bridging butadiene groups. To avoid the formation of oligomeric species, such as observed in the solid state for $[(C_5H_4)SiMe_2(N\text{-}t\text{-}Bu)]Zr(C_4H_6)$, a series of mononuclear Zr 1,4-diphenylbutadiene complexes, $[(Ring)SiMe_2(NR)]Zr(C_4H_4Ph_2)$, Ring = C_5H_4, C_5Me_4, C_9H_6; R = *i*-Pr or *t*-Bu, were prepared. The results of our X-ray structural analyses have provided the opportunity to evaluate the stereoelectronic influence of the type of cyclopentadienyl functionality and the size of the alkyl substituent, R, on the relative importance of the η^4-π diene and the η^2-σ^2,π diene representations for the metal−butadiene bonding interaction.

Results and Discussion

Synthesis and Characterization of Several *ansa*-Monocyclopentadienylamido-Type Zr Dichloride Complexes. The attachment of a bifunctional monocyclopentadienyldimethylsilylamido-type ligand to Zr is conveniently carried out by the thermally induced amine elimination reaction of $(RingH)SiMe_2(NHR)$ with $Zr(NMe_2)_4$ (eq 1). For Ring = C_5H_4, C_5Me_4 and R = *i*-Pr, *t*-Bu, this reaction is best performed by heating a neat 1:1 reaction mixture while purging the released NMe_2H with nitrogen. As these reactions proceed to completion, the $[(Ring)SiMe_2(NR)]Zr(NMe_2)_2$ complexes are sufficiently volatile to collect on the upper cool portion of the reaction flask and may be readily purified by sublimation. In contrast, the neat amine elimination reaction of $(C_9H_7)SiMe_2(NH\text{-}t\text{-}Bu)$ with $Zr(NMe_2)_4$ affords a dark orange, viscous oil.[9] These bis(dimethylamido) Zr intermediates were identified by solution NMR measurements.

The $[(Ring)SiMe_2(NR)]Zr(NMe_2)_2$ complexes are readily converted to $[(Ring)SiMe_2(NR)]ZrCl_2$ by heating the respective toluene solution in the presence of excess $SiMe_3Cl$ overnight at 60 °C (eq 2). These reactions proceed with elimination of NMe_2SiMe_3, which is readily removed under vacuum. The overall yields obtained from this two-step reaction sequence range from 70 to 85% for $[(C_5H_4)SiMe_2(N\text{-}t\text{-}Bu)]ZrCl_2$, **1**, $[(C_9H_6)SiMe_2(N\text{-}t\text{-}Bu)]ZrCl_2$, **2**, $[(C_5Me_4)$-

(6) (a) Okuda, J. *Chem. Ber.* **1990**, *123*, 1649−1651. (b) Okuda, J.; Schattenmann, F. J.; Wocadlo, S.; Massa, W. *Organometallics* **1995**, *14*, 789−795. (c) Okuda, J. In *Metallocenes*; Togni, A., Halterman, R. L., Eds.; Wiley-VCH: Weinheim, 1999; pp 415−450 and references therein.

(7) Strickler, J. R.; Power, J. M. U.S. Patent 5,359,105, 1994.

(8) (a) Hughes, A. K.; Meetsma, A.; Teuben, J. H. *Organometallics* **1993**, *12*, 1936−1945. (b) Sinnema, P.-J.; van der Veen, L.; Spek, A. L.; Veldman, N.; Teuben, J. H. *Organometallics* **1997**, *16*, 4245−4247.

(9) Hermmann, W. A.; Morawietz, M. J. A. *J. Organomet. Chem.* **1994**, *482*, 169−181.

(10) Carpenetti, D. W.; Kloppenburg, L.; Kupec, J. T.; Petersen, J. L. *Organometallics* **1996**, *15*, 1572−1581.

(11) Leung, W.-P.; Song, F.-Q.; Zhou, Z.-Y.; Xue, F.; Mak, T. C. W. *J. Organomet. Chem.* **1999**, *575*, 232−241.

(12) Kloppenburg, L. Ph.D. dissertation, University of Münster, 1997.

(13) Brenner, S.; Kempe, R.; Arndt, P. *Z. Anorg. Allg. Chem.* **1995**, *621*, 2021−2024.

(14) (a) Sinnema, P.-J.; Liekelema, K.; Stall, O. K. B.; Hessen, B.; Teuben, J. H. *J. Mol. Catal.* **1998**, *128*, 143−153. (b) Sinnema, P.-J. Ph.D. dissertation, University of Gröningen, 1999.

(15) (a) Devore, D. D.; Timmers, F. J.; Hasha, D. L.; Rosen, R. K.; Marks, T. J.; Deck, P. A.; Stern, C. L. *Organometallics* **1995**, *14*, 3132−3134. (b) Devore, D. D.; Stevens, J. C.; Timmers, F. J.; Rosen, R. K. U.S. Patent 5,539,068, 1996.

(16) (a) Cowley, A. H.; Hair, G. S.; McBurnett, B. G.; Jones, R. A. *J. Chem. Soc., Chem. Commun.* **1999**, 437−438. (b) Hair, G. S.; Jones, R. A.; Cowley, A. H.; Lynch, V. *Inorg. Chem.* **2001**, *40*, 1014−1019.

(17) Dahlmann, M.; Schottek, J.; Fröhlich, R.; Kunz, D.; Nissinen, M.; Erker, G.; Fink, G.; Kleinschmidt, R. *J. Chem. Soc., Dalton Trans.* **2000**, 1881−1886.

(18) Strauch, J. W.; Petersen, J. L. *Organometallics* **2001**, *20*, 2623−2630.

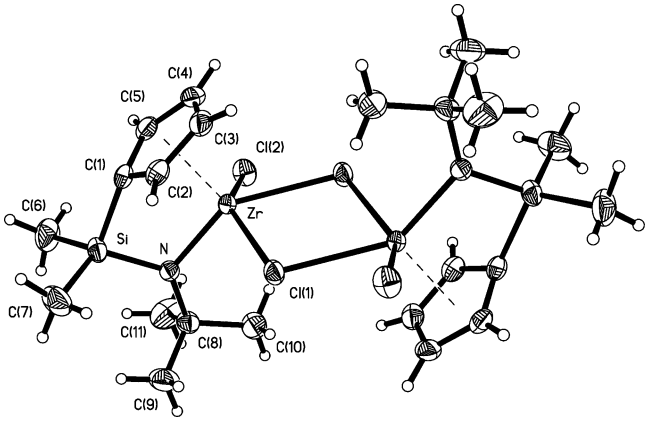

Figure 1. Perspective view and the atom labeling scheme for the dimeric structure of $[(C_5H_4)SiMe_2(N\text{-}t\text{-}Bu)]ZrCl_2$, **1**. The thermal ellipsoids are scaled to enclose 30% probability. This dimeric structure is constrained by a crystallographic center of inversion.

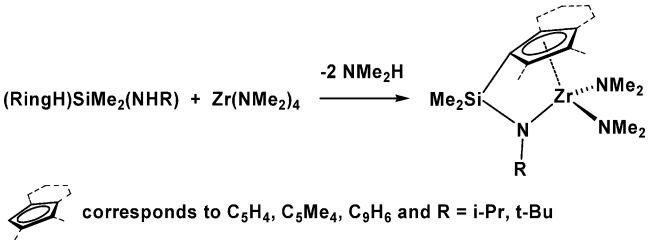

$SiMe_2(N\text{-}i\text{-}Pr)]ZrCl_2$, **3**, and $[(C_5Me_4)SiMe_2(N\text{-}t\text{-}Bu)]ZrCl_2$. $[(C_5Me_4)SiMe_2(N\text{-}t\text{-}Bu)]ZrCl_2$ and **2** may be purified by sublimation, whereas compounds **1** and **3** were recrystallized by cooling a hot toluene solution. These four compounds were characterized by ^1H and ^{13}C NMR measurements, and their molecular structures were verified by X-ray crystallography.

The solution NMR spectra of **1** and **3** exhibit mirror symmetry consistent with the presence of mononuclear structures in solution. The introduction of the indenyl group in **2** results in the appearance of two well-separated sets of proton and carbon resonances for the inequivalent methyl substituents of the dimethylsilyl bridge. Whereas the mononuclear structure of **2** is retained in the solid state, the molecular structures of **1** and **3** are centrosymmetric dimers, held together by a pair of bridging Cl ligands. Perspective views of the molecular structures of **1**, **2**, and **3** are depicted in Figures 1, 2, and 3, respectively, with the atom labeling scheme provided for the independent nonhydrogen atoms.

The coordination geometry about each Zr atom in **1** and **3** resembles a four-legged piano stool, with the appended amido N atom trans to the inner bridging Cl_{inner} atom and the terminal Cl_t (i.e. Cl(2)) atom disposed opposite to the outer bridging Cl_{outer} (i.e., Cl(1)). In **1**, the Zr atom is disposed

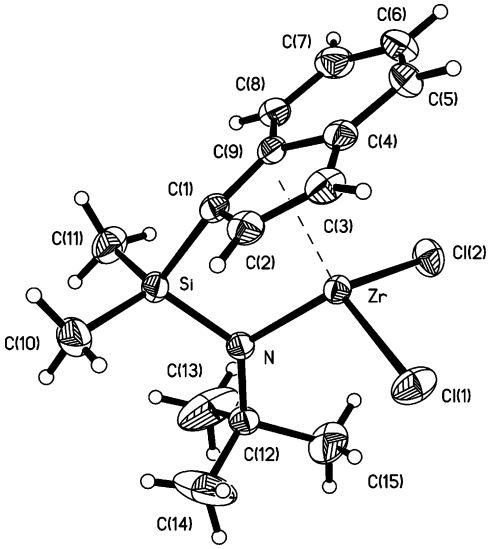

Figure 2. Perspective view of the molecular structure and the atom labeling scheme for $[(C_9H_6)SiMe_2(N\text{-}t\text{-}Bu)]ZrCl_2$, **2**. The thermal ellipsoids are scaled to enclose 30% probability.

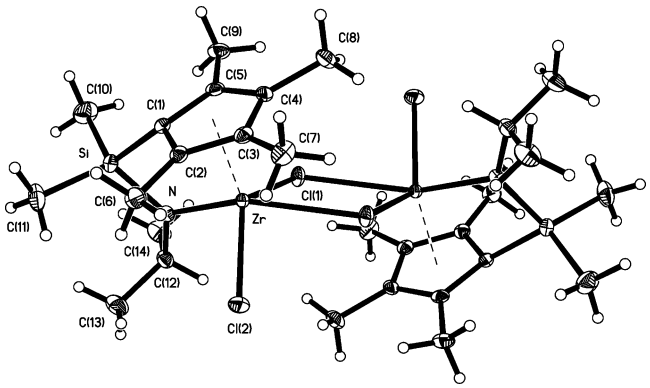

Figure 3. Perspective view and the atom labeling scheme for the dimeric structure of $[(C_5Me_4)SiMe_2(N\text{-}i\text{-}Pr)]ZrCl_2$, **3**. The thermal ellipsoids are scaled to enclose 30% probability. This dimeric structure is constrained by a crystallographic center of inversion.

0.689 Å from the plane defined by the terminal Cl atom, the two bridging Cl atoms, and the amido N atom. In contrast, because the $N-Zr-Cl_{inner}$ angle is ca. 30° greater than the $Cl_t-Zr-Cl_{outer}$ angle in **3**, the two legs defined by the Zr−N and $Zr-Cl_{inner}$ bond vectors are directed farther away from each other, whereas the other two legs defined by the $Zr-Cl_t$ and $Zr-Cl_{outer}$ bond vectors are more disposed toward one another than in **1**.

The Zr−Cl bond distances for the outer and inner bridging chlorides within the central $Zr_2(\mu\text{-}Cl)_2$ moiety of **1** are 2.618(1) and 2.657(1) Å with a terminal $Zr-Cl_t$ distance of 2.453(1) Å. The corresponding bridging Zr−Cl distances in **3** of 2.542(1) and 2.745(1) Å reflect a substantially higher degree of asymmetry. A comparable level of asymmetry exists in *RR*-$\{[(C_5Me_4)SiMe_2(NCH(Me)Ph)]ZrCl(\mu\text{-}Cl)\}_2$,[11] with the two outer bridging Zr−Cl bonds being 2.541(2) and 2.547(2) Å and the two inner bridging Zr−Cl bonds being 2.760(2) and 2.807(2) Å for the nearly planar $Zr_2(\mu\text{-}Cl)_2$ core. The weaker dative $Zr\leftarrow Cl_{inner}$ interaction of **3** is compensated by a 0.076 Å decrease in the $Zr-Cl_{outer}$ distance and a 0.02 Å reduction of the $Zr-Cl_t$ distance to 2.434(1) Å and is accompanied by a ca. 10° increase in the $N-Zr-Cl_{inner}$ angle

from 144.48(7) to 154.33(8)° and a ca. 19° decrease in the $Cl_t-Zr-Cl_{outer}$ angle from 143.38(3) to 124.62(4)° for **1** and **3**, respectively. The perpendicular displacements of the terminal Cl ligands from the planar $Zr_2(\mu\text{-}Cl)_2$ core are 1.06 and 1.81 Å for **1** and **3**, respectively.

In contrast, the four-coordinate geometry of **2** resembles that of a distorted tetrahedron and is similar to that displayed by $[(C_5Me_4)SiMe_2(N\text{-}t\text{-}Bu)]ZrCl_2$.[10] The position of the indenyl group is such that the plane passing through the bridgehead C, Si, and N atoms bisects the Cl−Zr−Cl angle. The replacement of the indenyl group of **2** with the better π-donating C_5Me_4 ring[19] leads to a ca. 0.03 Å decrease in the Zr−Cp(c) distance, a 0.01 Å increase in the Zr−N(amido) distance, and a pair of nearly equal Zr−Cl bonds. However, the lower coordination number and formal electron count of Zr in **2** and $[(C_5Me_4)SiMe_2(N\text{-}t\text{-}Bu)]ZrCl_2$ allow the Cl ligands to π donate more effectively to the electrophilic Zr, thus producing a 0.04−0.06 Å decrease in their corresponding Zr−Cl bond distances.

The X-ray crystallographic data of compounds **1**, **2**, and **3** reflect the structural changes that occur during the transition from a symmetric dimer, **1**, through an intermediate asymmetric dimer, **3**, to two non-interacting, well-separated four-coordinate monomers, such as observed for **2** and $[(C_5Me_4)SiMe_2(N\text{-}t\text{-}Bu)]ZrCl_2$. Dissociation of the symmetric dimer proceeds with elongation of the $Zr-Cl_{inner}$ distance and with concomitant reduction in the $Cl_t-Zr-Cl_{outer}$ angle and the $Zr-Cl_{outer}$ distance. As this process proceeds with further weakening of the dative $Zr\leftarrow Cl_{inner}$ interaction, the $Cl_t-Zr-Cl_{outer}$ bond angle approaches 105°, and the difference in the $Zr-C_t$ and $Zr-Cl_{outer}$ distances diminishes as their respective values approach 2.40 Å, a typical value for a terminal Zr−Cl bond distance in 14-electron, four-coordinate, monocyclopentadienyl Zr complexes.[20,21]

General Synthesis of $[(Ring)SiMe_2(NR)]Zr(C_4H_4Ph_2)$ Complexes (Ring = C_5H_4, C_5Me_4, and C_9H_6; R = *t*-Bu, *i*-Pr). The metathetical reactions of $[(Ring)SiMe_2(NR)]ZrCl_2$ (Ring = C_5H_4, C_5Me_4, C_9H_6; R = *t*-Bu, *i*-Pr) with a 5% excess of 1,4-diphenylbutadiene magnesium were carried out in toluene (eq 3). As each reaction proceeded, the color of the reaction mixture became dark red. The resultant 1,4-diphenylbutadiene compounds, $[(Ring)SiMe_2(NR)]Zr(C_4H_4Ph_2)$, were soluble in toluene, moderately soluble in pentane, and only modestly soluble in hexamethyldisiloxane. Purification of these butadiene compounds was accomplished by recrystallization from toluene or pentane, leaving dark red crystals. The identity of each compound was verified by solution ^1H and ^{13}C NMR measurements, and the peak assignments were made by examination of the observed cross-peaks in the corresponding 2D HETCOR and COSY NMR spectra.

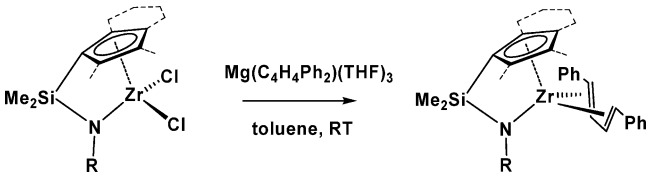

Characterization of the 1,4-Diphenylbutadiene Zr Complexes. The solution NMR data for $[(C_5H_4)SiMe_2(N\text{-}t\text{-}Bu)]Zr(C_4H_4Ph_2)$, **4**, and $[(C_5Me_4)SiMe_2(NR)]Zr(C_4H_4Ph_2)$, R = *i*-Pr (**6**), *t*-Bu (**7**), are consistent with the presence of mirror symmetry. The indenyl group in $[(C_9H_6)SiMe_2(N\text{-}t\text{-}Bu)]Zr(C_4H_4Ph_2)$, **5**, makes this compound chiral, as evidenced by the appearance of well-separated proton and carbon resonances for the two methyl substituents of the $SiMe_2$ bridge. For **4**, **6**, and **7**, the chemically equivalent meso and anti protons of each 1,4-diphenylbutadiene ligand produce two well-separated multiplets, consistent with an AA′XX′ coupling system. The independent J_{H-H} coupling constants were determined by computer simulation.[22] The magnitude of the $^3J_{meso-meso}$ and $^3J_{meso-anti}$ coupling constants of 10−12 Hz is consistent with a *cis*- rather than a *trans*-butadiene backbone.[23] The splitting patterns for the meso and anti protons of **4**, **6**, and **7** are similar and resemble the one that is simulated in Figure 4a. The loss of mirror symmetry in **5** leads to the appearance of two second-order multiplets centered at δ 6.16 and 6.10 for the chemically inequivalent meso protons of its major isomer, as shown in Figure 4b, and of two well-separated pseudo doublets of doublets for the chemically inequivalent anti protons. The corresponding ortho, meta, and para protons of the phenyl rings of **4**, **5**, **6**, and **7** exhibit an AA′BB′C splitting pattern with six independent coupling constants. The J_{H-H} coupling constants between the ortho, meta, and para phenyl ring protons were also determined by computer simulation.[22]

The ^1H NMR spectra reveal that compound **6** exhibits one primary species in solution, whereas compounds **4**, **5**, and **7** afford >20:1, 6:1, and 2:1 mixtures, respectively, of two conformational isomers, which differ in terms of the orientation of the butadiene cup with respect to the cyclopentadienyl functionality. The supine structure has the open end of the diene cup directed toward the cyclopentadienyl functionality, whereas the alternative prone structure has the opening of the diene cup directed away from the cyclopentadienyl ring. The magnitude of the chemical shift difference, $\Delta\delta_H$, between the downfield meso (δ_{meso}) and upfield anti (δ_{anti}) protons of the *cis*-butadiene of the supine structure is typically 2−3 times greater than that for the prone isomer. The chemical shifts of the meso and anti butadiene protons of **4** (major and minor), **5** (major and minor), **6**, and **7** (major and minor) and the J_{H-H} coupling constants are summarized in Table 1. The range of the chemical shift difference observed for **4** (major), **5** (major), **6**, and **7** (major) is 4.3−5.0 ppm, which

(19) (a) Gassman, P. G.; Winter, C. H. *J. Am. Chem. Soc.* **1988**, *110*, 6130−6135. (b) Richardson, D. E.; Alameddin, N. G.; Ryan, M. F.; Hayes, T.; Eyler, J. R.; Siedle, A. R. *J. Am. Chem. Soc.* **1996**, *118*, 11244−11253.

(20) Pupi, R. M.; Coalter, J. N.; Petersen, J. L. *J. Organomet. Chem.* **1995**, *497*, 17−25.

(21) Yue, N.; Hollink, E.; Guerin, F.; Stephan, D. W. *Organometallics* **2001**, *20*, 4424−4433.

(22) SpinWorks, version 2.1 (Professor Kirk Marat, Department of Chemistry, University of Manitoba, Manitoba, Canada R3T 2N2), permits off-line processing of 1D and 2D NMR data and may be used for the simulation and analysis of complex second-order spectra and dynamic NMR spectral data.

(23) Benn, R.; Schroth, G. *J. Organomet. Chem.* **1982**, *228*, 71−85.

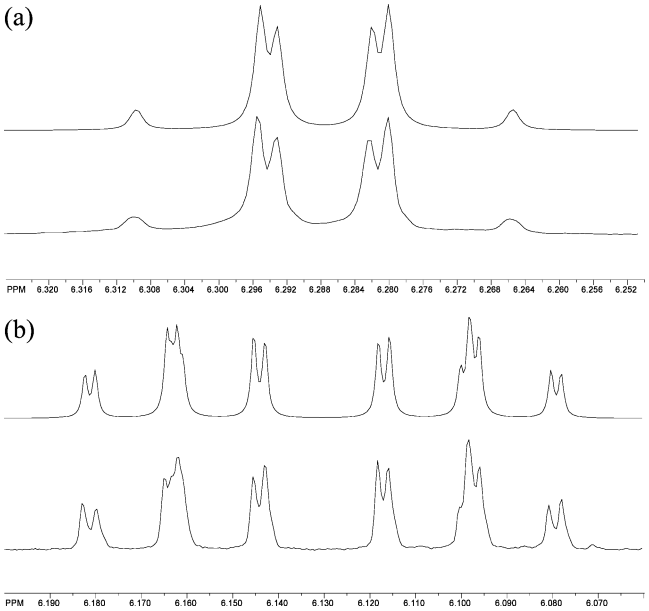

Figure 4. (a) Simulated (top) and experimental (bottom) AA′XX′ splitting pattern observed for the chemically equivalent *meso*-butadiene protons of **4** (major) and (b) simulated (top) and experimental (bottom) second-order splitting pattern observed for the chemically inequivalent *meso*-butadiene protons of **5** (major).

is substantially larger than the $\Delta\delta_H$ range of 2.2−2.4 ppm for the minor isomers of **4**, **5**, and **7**. On the basis of these solution NMR data, compounds **4** (major), **5** (major), **6**, and **7** (major) conform to the supine structure, whereas **4** (minor), **5** (minor), and **7** (minor) are assigned to the alternative prone structure.

Description of the Molecular Structures of the 1,4-Diphenylbutadiene Zr Complexes. The molecular structures of [$(C_5H_4)SiMe_2$(N-*t*-Bu)]Zr($C_4H_4Ph_2$), **4**, [$(C_9H_6)SiMe_2$(N-*t*-Bu)]Zr($C_4H_4Ph_2$), **5**, [$(C_5Me_4)SiMe_2$(N-*i*-Pr)]Zr($C_4H_4Ph_2$), **6**, and [$(C_5Me_4)SiMe_2$(N-*t*-Bu)]Zr($C_4H_4Ph_2$), **7**, were determined by analyses of X-ray diffraction data collected while cooling the samples at −50 °C (Table 2). The crystals used for these structural analyses were grown at ambient temperature by slow removal of solvent from a saturated solution of the respective compound. Perspective views of the molecular structures with the appropriate atom labeling scheme are depicted in Figures 5, 6, 7, and 8, respectively.

The Zr coordination environment in each complex is comprised of the π-bonded cyclopentadienyl ring functionality, the anionic amido N-donor of the corresponding bifunctional ligand, and a 1,4-diphenylbutadiene moiety. The open cup of the *cis*-diene ligand is directed toward the cyclopentadienyl functionality, consistent with the supine conformation. The metal−diene bonding interaction and spatial orientation of the diene unit are compatible with the structures reported by Erker and co-workers[17] for [$(C_5Me_4)SiMe_2$(NCHMe(1-$C_{10}H_7$))]Zr(C_4H_6) and the major isomer of [$(C_5Me_4)SiMe_2$(N-*t*-Bu)]Zr(C_4H_6) and by Strauch and Petersen[18] for [$(C_5Me_4)SiMe_2$(N-*i*-Pr)]Zr(C_4H_6). The planar phenyl substituents of the *cis*-diene ligand in **4**−**7** are directed laterally from the terminal butadiene carbons, with their planes rotated 25−40° from being coplanar with the plane defined by the four central carbons of the coordinated diene.

Two representations, η^4-π diene and η^2-σ^2,π diene, have been invoked to describe the nature of the metal−butadiene bonding interaction. Two different approaches have been used to evaluate the relative importance of these two representations from an examination of the X-ray crystallographic data. Erker and co-workers[24] observed for a series of Group 4 metallocene butadiene complexes that η^4-π diene complexes are recognized by shorter M−C(internal) and C(terminal)−C(internal) bond distances and by smaller M−C(terminal)−C(internal) bond angles than the values of these three parameters in η^2-σ^2,π diene complexes. For example, the corresponding values of 2.550(5) Å, 1.445(2) Å, and 81.8(1)° for Cp_2Zr(η^4-1,2,5,6-tetramethyl-3,4-dimethylenetricyclo[3.1.0.$0^{2.6}$]hexane)[24b] are compatible with the η^4-π diene representation, whereas the substantially larger values of 2.885(4) Å, 1.48(1) Å, and 95.8° for Cp_2Zr-(indanediyl)[25] are indicative of a pure η^2-σ^2 interaction lacking a π-bonding component. From their examination of the values of these three structural parameters for M(η^4-C_4H_6)Ph[$N(SiMe_2CH_2PMe_2)_2$] (M = Zr, 2.466(11) Å, 1.42(2) Å, 76.3(7)°; M = Hf, 2.456(7) Å, 1.429(12) Å, 76.5(5)°), Fryzuk and co-workers[26] concluded that these two complexes exhibit a higher degree of η^4-π character than that found in Group 4 metallocene diene complexes. The corresponding structural data (2.400(5) Å, 1.437(8) Å, 73.6° (av)) for the Hf dibutadiene complex, Hf(C_4H_6)$_2$(dmpe),[27] also reflect the prevalence of the η^4-π diene interaction.

The alternative approach[28] used to evaluate the nature of the metal−diene bonding interaction involves a correlation between the dihedral angle, α (defined as the angle between the plane passing through the four diene carbons and the plane through the metal and two terminal carbons of the diene), and the ΔM−C distance (defined as the difference between the average of the pair of M−C(terminal) and M−C(internal) bond distances). Group 4 metallocene complexes with appreciable η^4-π diene character[24] typically exhibit values of α > 110°, with ΔM−C varying from −0.3 to −0.5 Å. For late-transition-metal η^4-π diene complexes, the values of α and ΔM−C typically range from 75 to 90° and from −0.1 to 0.1 Å, respectively.[28] The values of α and ΔM−C observed for M = Zr of 98.9° and −0.171 Å and for M = Hf of 97.5° and −0.193 Å in M(η^4-C_4H_6)Ph[N-($SiMe_2CH_2PMe_2)_2$][26] provide further indication of greater η^4-π character than that in Group 4 metallocene diene complexes.

(24) (a) Erker, G.; Krüger, C.; Müller, G. *Adv. Organomet. Chem.* **1985**, *24*, 1−39. (b) Erker, G.; Engel, K.; Krüger, C.; Müller, G. *Organometallics* **1984**, *3*, 128−133. (c) Krüger, C.; Müller, G.; Erker, G.; Dorf, U.; Engel, K. *Organometallics* **1985**, *4*, 215−223. (d) Erker, G.; Engel, K.; Krüger, C.; Chiang, A.-P. *Chem. Ber.* **1982**, *115*, 3311−3323. (e) Erker, G.; Wicher, J.; Engel, K.; Rosenfeldt, F.; Dietrich, W.; Krüger, C. *J. Am. Chem. Soc.* **1980**, *102*, 6346−6348.
(25) Lappert, M. F.; Martin, T. R.; Atwood, J. L.; Hunter, W. E. *J. Chem. Soc., Chem. Commun.* **1980**, 476−477.
(26) Fryzuk, M. D.; Haddad, T. S.; Rettig, S. J. *Organometallics* **1989**, *8*, 1723−1732.
(27) Wreford, S. S.; Whitney, J. F. *Inorg. Chem.* **1981**, *20*, 3918−3924.
(28) (a) Yasuda, H.; Nakamura, A.; Kai, Y.; Kasai, N. *Topics in Physical Organometallic Chemistry*; Freund Publishing House: Tel Aviv, 1987; Vol. 2. (b) Yasuda, H.; Tatsumi, K.; Okamoto, T.; Mashima, K.; Lee, K.; Nakumura, A.; Kai, Y.; Kanehisa, N.; Kasai, N. *J. Am. Chem. Soc.* **1985**, *107*, 2410−2422.

Table 1. Summary of ^{1}H NMR Data for the Meso and Anti Protons of the 1,4-Diphenylbutadiene Ligands in **4**−**7**

compound	structure	δ_{meso}	δ_{anti}	J(H−H), Hz[a]
4 (major)	supine	6.28	1.97	J(m−m′) = 9.94(6), J(m−a′) = −2.12(8), J(a−a′) = 0.22(5), J(a−m) = 11.18(1)
4 (minor)	prone	5.12	2.70	J(m−m′) = 11.44(7), J(m−a′) = −1.8(1), J(a−a′) = 0.29(6), J(a−m) = 12.59(1)
5 (major)	supine	6.15 (m_1)	1.72 (a_1)	$J(m_1-m_2)$ = 10.70(7), $J(m_1-a_2)$ = 1.34(7), $J(m_2-a_1)$ = 1.17(7),
		6.11 (m_2)	1.25 (a_2)	$J(a_1-a_2)$ = 0.16(7), $J(m_1-a_1)$ = 11.84(7), $J(m_2-a_2)$ = 12.03(7)
5 (minor)	prone	5.31 (m_1)	2.58 (a_1)	$J(m_1-m_2)$ = 11.5(2), $J(m_1-a_2)$ = 1.6(2), $J(m_2-a_1)$ = 1.3(2),
		4.42 (m_2)	2.43 (a_2)	$J(a_1-a_2)$ = 0.2(2), $J(m_1-a_1)$ = 12.3(2), $J(m_2-a_2)$ = 12.5(2)
6	supine	6.22	1.70	J(m−m′) = 10.77(5), J(m−a′) = −2.26(7), J(a−a′) = 0.60(4), J(a−m) = 10.96(1)
7 (major)	supine	6.38	1.37	J(m−m′) = 10.55(7), J(m−a′) = −2.2(1), J(a−a′) = 0.43(6), J(a−m) = 11.28(1)
7 (minor)	prone	5.01	2.83	J(m−m′) = 11.41(9), J(m−a′) = −1.5(1), J(a−a′) = 0.24(7), J(a−m) = 13.05(3)

[a] The esd's determined from the computer simulation are given in parentheses.

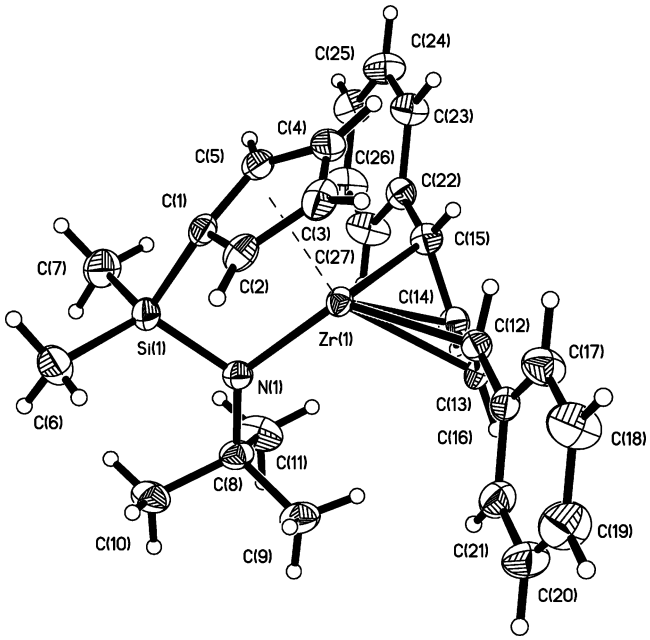

Figure 5. Perspective view of molecular structure of the supine isomer of [$(C_5H_4)SiMe_2$(N-*t*-Bu)]Zr($C_4H_4Ph_2$), **4**, and the atom labeling scheme. The thermal ellipsoids are scaled to enclose 30% probability.

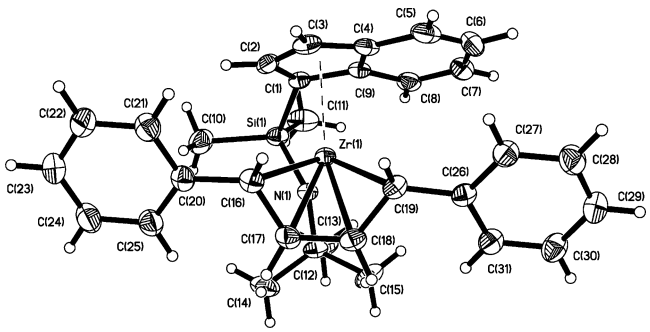

Figure 6. Frontal view of the molecular structure of the supine isomer of [$(C_9H_6)SiMe_2$(N-*t*-Bu)]Zr($C_4H_4Ph_2$), **5**, and the atom labeling scheme. The thermal ellipsoids are scaled to enclose 30% probability.

The structural data summarized in Table 4 indicate that the four Zr−1,4-diphenylbutadiene complexes **4**−**7** also exhibit pronounced η^4-π diene character. The average Zr−C(internal) distances range from 2.42 to 2.46 Å, the average C(terminal)−C(internal) distances vary from 1.4 to 1.46 Å, and the average Zr−C(terminal)−C(internal) bond angles fall between 69 and 79°. The five-membered ZrC_4 moieties are appreciably folded with the dihedral angle, α, ranging from 100° (**6**) to 110.8° (**7**). The substantial folding of this molecular unit places all four butadiene carbons within a bonding distance of the electrophilic Zr center, thus resulting in ΔZr−C values varying from −0.09 Å (**6**) to −0.14 Å (**7**). The smallest dihedral angle, α, is accompanied by the smallest ΔZr−C value, and vice versa. The methine H atom of the isopropyl substituent on the amido N of **6** is directed toward the diene ligand. Consequently, the replacement of the *tert*-butyl substituent in **7** with the sterically less demanding isopropyl group enhances the π-bonding contribution to the Zr−diene interaction and affords greater π-donation from the amido N donor. The resultant structural adjustments include a 0.03 Å decrease in the average Zr−C(internal) bond distance, a nearly 11° decrease in the dihedral angle, α, and a 0.035 Å decrease in the Zr−N bond distance.

Coordination of a cis η^4-π diene to an electrophilic metal often leads to a long−short−long sequence for the three C−C bonds within the butadiene ligand.[24,26−28] With the exception of **7**, the central C−C bond is 0.04−0.07 Å shorter than the outer two C−C bonds of the coordinated diene. Compound **6**, which has the smallest dihedral angle, α, and shortest pair of Zr−C(internal) distances, also exhibits the shortest internal C−C bond distance of 1.374(5) Å. This long−short−long C−C bond variation may be rationalized by treating **4**−**7** as Zr(II) η^4-diene rather than as Zr(IV) enediyl complexes. On the basis of the former description, one anticipates that as the dihedral angle, α, decreases toward 90°, the degree of π-back-donation from the filled Zr-d_π orbital to the empty lower-lying π^* antibonding orbital of the neutral diene should increase. Because the two nodes in this diene π^* orbital lie between the C(terminal)−C(internal) bonds, an increase in π-back-donation would be expected to enhance the long−short−long variation of the C−C distances within the coordinated diene. The structural data provided in Table 4 are consistent with this description.

The Zr−C(terminal) bond distances in these butadiene complexes range from 2.30 to 2.35 Å and are modestly longer than the corresponding values of 2.300 (av), 2.300(5), and 2.278(6) Å observed in [$(C_5Me_4)SiMe_2$(NCHMe-(1-$C_{10}H_7$))]Zr(C_4H_6),[17] [$(C_5Me_4)SiMe_2$(N-*t*-Bu)]Zr(C_4H_6),[17] and [$(C_5Me_4)SiMe_2$(N-*i*-Pr)]Zr(C_4H_6),[18] respectively, which are more typical of a Zr−C σ-bond. For example, the bond distances for the Zr−C σ-bonds in $(C_5H_5)_2ZrMe_2$ and $(C_9H_6)_2$-$ZrMe_2$ are 2.273(5), 2.280(5)[29] and 2.251(6) Å,[30] respectively.

(29) Hunter, W. E.; Hrncir, D. C.; Vann Bynum, R.; Penttila, R. A.; Atwood, J. L. *Organometallics* **1983**, *2*, 750−755.
(30) Atwood, J. L.; Hunter, W. E.; Hrncir, D. C.; Samuel, E.; Alt, H.; Rausch, M. D. *Inorg. Chem.* **1975**, *14*, 1757−1762.

Table 2. X-ray Data for {[(C_5H_4)$SiMe_2$(N-*t*-Bu)]ZrCl_2(μ-Cl)}$_2$, **1**, [(C_9H_6)$SiMe_2$(N-*t*-Bu)]$ZrCl_2$, **2**, {[(C_5Me_4)$SiMe_2$(N-*i*-Pr)]ZrCl(μ-Cl)}$_2$, **3**, [(C_5H_4)$SiMe_2$(N-*t*-Bu)]Zr($C_4H_4Ph_2$), **4**, [(C_9H_6)$SiMe_2$(N-*t*-Bu)]Zr($C_4H_4Ph_2$), **5**, [(C_5Me_4)$SiMe_2$(N-*i*-Pr)]Zr($C_4H_4Ph_2$), **6**, and [(C_5Me_4)$SiMe_2$(N-*t*-Bu)]Zr($C_4H_4Ph_2$), **7**

	1	**2**	**3**	**4**	**5**	**6**	**7**
				A. Crystal Data			
empirical formula	$C_{11}H_{19}Cl_2NSiZr$	$C_{15}H_{21}Cl_2NSiZr$	$C_{14}H_{25}Cl_2NSiZr$	$C_{27}H_{33}NSiZr\cdot 1/2C_7H_8$	$C_{31}H_{35}NSiZr\cdot 1/2C_7H_8$	$C_{30}H_{39}NSiZr$	$C_{31}H_{41}NSiZr$
crystal dimensions, mm	0.16 × 0.20 × 0.50	0.20 × 0.30 × 0.44	0.22 × 0.32 × 0.34	0.06 × 0.18 × 0.44	0.10 × 0.14 × 0.75	0.04 × 0.16 × 0.32	0.14 × 0.18 × 0.20
crystal system	triclinic	monoclinic	triclinic	monoclinic	monoclinic	monoclinic	monoclinic
space group	$P\bar{1}$	$P2_1/n$	$P\bar{1}$	$P2_1/c$	$P2_1/c$	$P2_1$	$P2_1/n$
a, Å	7.5702(7)	8.389(1)	8.788(1)	12.969(2)	13.433(1)	12.473(2)	8.106(1)
b, Å	8.4119(8)	23.430(4)	10.061(1)	8.081(1)	8.2506(5)	8.813(1)	27.937(3)
c, Å	13.0173(15)	9.254(2)	11.842(2)	26.723(4)	27.696(2)	12.562(2)	12.872(1)
α, deg	92.43(1)	90	94.81(1)	90	90	90	90
β, deg	103.75(1)	90.42(1)	110.94(1)	96.626(3)	100.977(1)	97.771(2)	102.009(2)
γ, deg	107.60(1)	90	110.16(1)	90	90	90	90
volume, Å^3	761.6(1)	1818.9(5)	892.0(2)	2782.0(8)	3013.4(3)	1368.2(3)	2851.0(5)
Z	2 monomer units/cell	4	2 monomer units/cell	4	4	2	4
emp. formula weight, amu	355.48	405.54	397.56	536.92	586.98	532.93	546.96
calcd density, g/cm^3	1.550	1.481	1.480	1.282	1.294	1.294	1.274
μ, cm^{-1}	11.28	9.55	9.71	4.56	4.28	4.63	4.46
F(0 0 0)	360	824	408	1124	1228	560	1152
temperature, °C	22 ± 1	22 ± 1	−80 ± 1	−50 ± 1	−50 ± 1	−50 ± 1	−50 ± 1
				B. Data Collection and Structural Analyses			
2θ range, deg	5.12−50.00	4.75−45.0	4.44−50.0	3.06−55.08	3.88−55.02	3.28−55.06	3.54−55.00
reflections sampled	$0 \le h \le 8$ $-9 \le k \le 9$ $-15 \le l \le 15$	$-1 \le h \le 9$ $-1 \le k \le 25$ $-9 \le l \le 9$	$-5 \le h \le 9$ $-11 \le k \le 11$ $-14 \le l \le 13$	$-16 \le h \le 16$ $-8 \le k \le 10$ $-34 \le l \le 34$	$-17 \le h \le 17$ $-8 \le k \le 10$ $-35 \le l \le 35$	$-15 \le h \le 16$ $-10 \le k \le 11$ $-16 \le l \le 16$	$-10 \le h \le 9$ $-36 \le k \le 34$ $-16 \le l \le 16$
no. of refl. collected	2859	3089	3680	19174	20661	9870	20264
no. of unique data	2640 (R_{int} = 0.0152)	2359 (R_{int} = 0.0173)	3016 (R_{int} = 0.0192)	6256 (R_{int} = 0.0854)	6734 (R_{int} = 0.0486)	4772 (R_{int} = 0.0436)	6511 (R_{int} = 0.0665)
no. of data, $I > 2\sigma(I)$	2381	1916	2590	3578	4926	4048	4297
a, *b*	0.0236, 0.6222	0.0362, 0.6112	0.0293, 0.6299	0.0344, 0.0000	0.0517, 0.3689	0.0215, 0.0000	0.0497, 0.3918
R indices, $I > 2\sigma(I)$	R1 = 0.0270, wR2 = 0.0668	R1 = 0.0303, wR2 = 0.0699	R1 = 0.0281, wR2 = 0.0649	R1 = 0.0551, wR2 = 0.0883	R1 = 0.0419, wR2 = 0.1008	R1 = 0.0347, wR2 = 0.0709	R1 = 0.0504, wR2 = 0.1144
R indices, all data	R1 = 0.0321, wR2 = 0.0764	R1 = 0.0443, wR2 = 0.0758	R1 = 0.0386, wR2 = 0.0699	R1 = 0.1243, wR2 = 0.1043	R1 = 0.0660, wR2 = 0.1099	R1 = 0.0472, wR2 = 0.0751	R1 = 0.0900, wR2 = 0.1286
σ_1, GOF	1.129	1.048	1.055	0.994	1.030	1.005	1.033
no. of variables	151	186	180	346	358	312	347
max. diff. peak and hole	0.245, −0.263	0.316, −0.244	0.426, −0.317	0.550, −0.471	0.455, −0.394	0.359, −0.439	0.589, −0.399

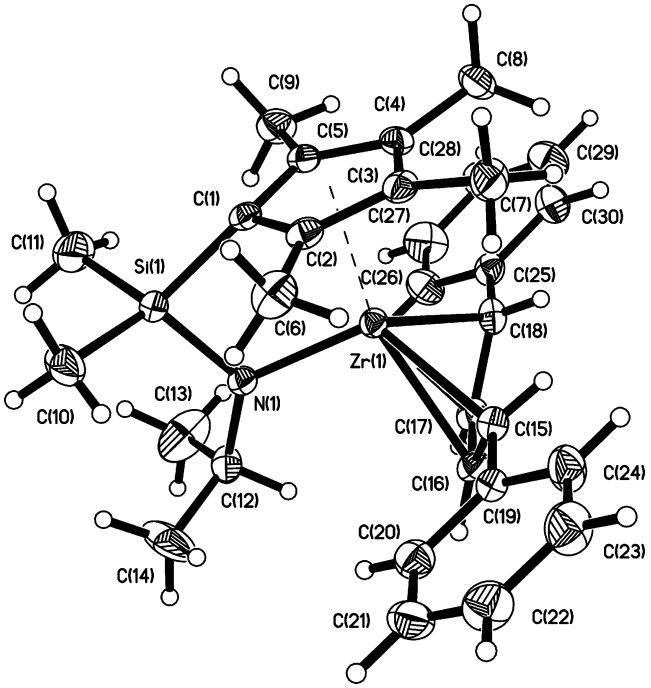

Figure 7. Perspective view of the molecular structure of the supine isomer of $[(C_5Me_4)SiMe_2(N\text{-}i\text{-}Pr)]Zr(C_4H_4Ph_2)$, **6**, and the atom labeling scheme. The thermal ellipsoids are scaled to enclose 30% probability.

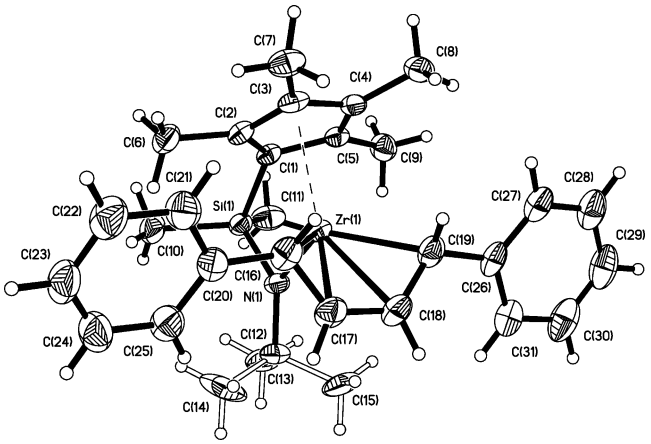

Figure 8. Perspective view of the molecular structure of the supine isomer of $[(C_5Me_4)SiMe_2(N\text{-}t\text{-}Bu)]Zr(C_4H_4Ph_2)$, **7**, and the atom labeling scheme. The thermal ellipsoids are scaled to enclose 30% probability. The methyl groups of the *tert*-butyl substituent suffer from a 75:25 two-site Star-of-David disorder. The atoms are only shown for the major site.

This modest increase in the Zr−C(terminal) bond distances may reflect an enhancement of the η^4-π diene contribution arising from the placement of a phenyl substituent at each terminal diene carbon. This remark is supported by a comparison of the pertinent structural parameters provided in Table 5 for $[(C_5Me_4)SiMe_2(N\text{-}i\text{-}Pr)]Zr(C_4H_6)$ and **6**. These data indicate that the introduction of the phenyl substituents leads to a lengthening of the Zr−C(terminal) bonds and a concomitant shortening of the corresponding Zr−C(internal) bonds, ultimately leading to a nearly 0.10 Å reduction in ΔZr−C. The subsequent decrease in the dihedral angle, α, from 110 to 100° is also accompanied by a more pronounced long−short−long C−C bond sequence.

Stephan and co-workers[21] recently reported that the related *cis*-diene complexes, $(C_5Me_5)Zr(NPR_3)(\eta^4$-2,3-dimethylbutadiene), where R = *i*-Pr, *t*-Bu, also exhibit the supine conformation. The respective values of α and ΔZr−C of 108.7°, −0.249 Å and of 116.5°, −0.377 Å are also consistent with an appreciable η^4-diene interaction in these two complexes. However, the shorter average Zr−C(terminal) distances of 2.285(3) and 2.263(6) Å, respectively,

Table 3. Selected Interatomic Distances (Å) and Bond Angles (°) for Complexes **1**−**3**

	1	**2**	**3**
	A. Interatomic Distances		
Zr−Cp(c)[a]	2.181	2.190	2.181
Zr−N	2.052(3)	2.042(3)	2.052(3)
Zr−Cl_t	2.453(1)	2.394(1), 2.400(1)	2.434(1)
Zr−Cl_{outer}	2.618(1)		2.542(1)
Zr−Cl_{inner}	2.657(1)		2.745(1)
Si−C_b[b]	1.866(4)	1.878(4)	1.874(3)
Si−N	1.734(3)	1.752(3)	1.730(3)
	B. Bond Angles		
Cp(c)−Zr−N	100.6	102.4	100.4
Cp(c)−Zr−Cl_t	109.2	114.2, 115.5	117.6
Cp(c)−Zr−Cl_{outer}	104.8		115.9
Cp(c)−Zr−C_{linner}	114.1		104.4
C_b−Si−N[b]	92.86(13)	93.1(2)	91.49(13)
N−Zr−Cl_t	95.69(8)	110.33(9), 109.19(9)	94.50(8)
N−Zr−Cl_{outer}	91.05(8)		89.10(8)
N−Zr−Cl_{inner}	144.48(7)		154.33(8)
Cl_t−Zr−Cl_t		105.21(5)	
Cl_t−Zr−Cl_{inner}	80.69(4)		79.75(3)
Cl_{inner}−Zr−Cl_{outer}	73.29(4)		74.35(4)
Cl_t−Zr−Cl_{outer}	143.38(3)		124.62(4)
Si−N−Zr	107.22(13)	106.0(2)	108.07(12)
C_a−N−Si[c]	129.0(2)	128.2(2)	129.8(2)
C_a−N−Zr[c]	123.6(2)	125.7(2)	122.1(2)

[a] Cp(c) corresponds to the centroid of the cyclopentadienyl ring. [b] C_b corresponds to the bridgehead carbon. [c] C_a corresponds to the carbon of the alkyl substituent at the amido nitrogen.

Table 4. Selected Interatomic Distances (Å) and Bond Angles (°) for Complexes **4**−**7**

	4	**5**	**6**	**7**
	A. Interatomic Distances			
Zr−Cp(c)[a]	2.173	2.198	2.170	2.195
Zr−N	2.086(3)	2.091(2)	2.074(3)	2.109(2)
Zr−C_1[b]	2.329(4)	2.308(2)	2.333(4)	2.301(3)
Zr−C_2	2.451(4)	2.444(2)	2.421(4)	2.448(3)
Zr−C_3	2.445(4)	2.465(2)	2.416(4)	2.459(3)
Zr−C_4	2.317(4)	2.347(2)	2.327(4)	2.324(2)
C_1−C_2	1.440(5)	1.436(3)	1.443(5)	1.393(4)
C_2−C_3	1.380(5)	1.393(3)	1.374(5)	1.403(4)
C_3−C_4	1.430(5)	1.474(3)	1.448(5)	1.400(4)
	B. Bond Angles			
Cp(c)−Zr−N	101.5	101.6	102.0	102.1
C_1−Zr−C_4	81.71(15)	82.06(7)	79.82(14)	84.19(9)
Si−N−Zr	103.96(14)	103.08(7)	105.47(15)	103.92(9)
C_b−Si−N[c]	94.8(2)	94.2(2)	93.5(2)	94.6(1)
Zr−C_1−C_2	77.2(2)	77.7(1)	69.0(2)	78.8(2)
C_1−C_2−C_3	125.9(4)	124.6(2)	124.3(3)	127.3(3)
C_2−C_3−C_4	124.8(4)	126.1(2)	123.7(3)	127.5(3)
C_3−C_4−Zr	77.5(2)	77.2(1)	68.9(2)	78.4(2)
C_{ipso}−C_1−Zr	132.6(3)	129.1(1)	129.9(3)	133.0(2)
C_{ipso}−C_4−Zr	128.2(3)	132.4(1)	128.7(3)	130.7(2)
C_{ipso}−C_1−C_2	123.4(4)	124.0(2)	123.0(3)	120.7(3)
C_{ipso}−C_4−C_3	125.1(4)	121.7(2)	122.8(3)	121.3(2)
dihedral angle, α	104.9	105.2	100.0	110.8

[a] Cp(c) corresponds to the centroid of the cyclopentadienyl ring. [b] C_1 and C_4 are the two terminal carbons and C_2 and C_3 represent the two internal carbons of the 1,4-diphenylbutadiene ligand. [c] C_b corresponds to the bridgehead carbon.

Table 5. Structural Parameters for $[(C_5Me_4)SiMe_2(N\text{-}i\text{-}Pr)]Zr(C_4H_4R_2)$; R = H, Ph

	$[(C_5Me_4)SiMe_2(N-i-Pr)]Zr(C_4H_6)$	**6**
Zr−C(terminal) (Å)	2.278(6)	2.330 (av)
Zr−C(internal) (Å)	2.463(5)	2.419 (av)
ΔZr−C[a] (Å)	−0.185	−0.089
C−C (outer) (Å)	1.413(7)	1.445 (av)
C−C (inner) (Å)	1.386(8)	1.374(5)
ΔC−C[b] (Å)	0.027	0.071
Zr−Cp(c) (Å)	2.163	2.170
Zr−N (Å)	2.117(6)	2.074(3)
dihedral angle, α (°)	110.0	100.0

[a] ΔZr−C corresponds to the difference between the Zr−C(terminal) and Zr−C(internal) bond distances. [b] ΔC−C corresponds to the difference between the C−C (outer) and C−C (inner) bond distances.

reflect a greater contribution from the σ^2,π-diene representation than observed in compounds **4**−**7**.

The bifunctional monocyclopentadienylamido ligands in **4**, **6**, and **7** are symmetrically disposed to afford structures with C_s symmetry, consistent with the NMR spectral data for these three compounds. The plane of symmetry passes through the bridgehead C, Si, N, and Zr atoms and the midpoint of the central C−C bond of the *cis*-diene ligand. Within each pair of shorter Zr−C(terminal) and longer Zr−C(internal) bonds, the bond distances are essentially equal. In contrast, the introduction of the unsymmetrical indenyl functionality in **5** leads to a significant lateral displacement of the $SiMe_2$ bridge. As a result, the plane passing through the bridgehead C, Si, and N atoms of **5** does not bisect the C(16)−Zr−C(19) bond angle. The perpendicular displacement of the Si atom from lying in the plane passing through the Zr and the midpoints of the central C(17)−C(18) bond and the C(16)···C(19) line segment of **5** is 1.207 Å. An analogous distortion is observed in the molecular structure of the Ti analogue, $[(C_9H_6)SiMe_2(N\text{-}t\text{-}Bu)]Ti(C_4H_4Ph_2)$, in which the η^4-π diene ligand adopts the alternative prone conformation.[31] The asymmetric coordination environment about the Zr atom of **5** is further reflected by a 0.04 Å difference in the two independent Zr−C(terminal) bond distances. The absence of mirror symmetry is consistent with the observation of four distinct proton and carbon resonances for the four chemically inequivalent H and C atoms of the central diene unit of **5**.

The structural analyses of **4**−**7** have shown that the *cis*-1,4-diphenylbutadiene ligand prefers the supine over the prone orientation. The level of the η^4-π bonding contribution is enhanced by replacement of the *t*-Bu substituent on the amido N atom with the sterically less demanding *i*-Pr group and is reflected by decreases in the dihedral angle, α, and ΔZr−C. The asymmetry introduced by the indenyl ligand leads to a lateral displacement of the $SiMe_2$ linker and a detectable variation in the two terminal Zr−C bond distances.

Experimental Section

Reagents. The hydrocarbon and ethereal solvents were purified by standard methods.[32] Toluene and pentane were refluxed over Na/K under a nitrogen flush and transferred to separate storage flasks containing $[(C_5H_5)_2Ti(\mu\text{-}Cl)_2]_2Zn$[33] or Na/K benzophenone ketyl. Hexamethyldisiloxane and diethyl ether were dried over $LiAlH_4$. The deuterated solvents C_6D_6 (Cambridge Isotopes, 99.5%) and $CDCl_3$ (Aldrich, 99.8%) were dried over activated 4A molecular sieves.

Starting materials such as $ZrCl_4$ (Alfa), $LiNMe_2$ (Aldrich, 95%), *n*-BuLi (Aldrich, 1.6 M in hexane), indene (Aldrich), *trans*-1,4-diphenylbutadiene (Aldrich), and 2,3-dimethyl-1,3-butadiene (Aldrich) were used without further purification. $SiMe_2Cl_2$ (Acros), $SiMe_3Cl$ (Acros), NH_2-*t*-Bu (Acros), and NH_2-*i*-Pr (Acros) were vacuum distilled prior to use and stored over 4A molecular sieves. $[(C_5H_4)SiMe_2(N\text{-}t\text{-}Bu)]Zr(NMe_2)_2$,[10] $[(C_5Me_4)SiMe_2(N\text{-}t\text{-}Bu)]ZrCl_2$,[10] $(C_9H_7)SiMe_2(N(H)\text{-}t\text{-}Bu)$,[9] $(C_5Me_4H)SiMe_2(N(H)\text{-}i\text{-}Pr)$,[34] and $Zr(NMe_2)_4$[35] were prepared using literature procedures.

Instrumentation. The ^{1}H NMR spectra of the zirconium dichloride compounds **1**, **2**, and **3** were measured with a JEOL Eclipse 270 MHz NMR spectrometer, whereas the ^{1}H NMR spectra of the zirconium 1,4-diphenylbutadiene compounds **4**, **5**, **6**, and **7** were measured with a Varian 600 Inova NMR spectrometer. All of the ^{13}C NMR spectra were measured with a JEOL Eclipse 270 NMR spectrometer, operating in the FT mode at 67.5 MHz. The ^{1}H chemical shifts are referenced to the residual proton peaks of benzene-d_6 at δ 7.15 (vs TMS) or chloroform-d_1 at δ 7.24 (vs TMS), whereas the central peak of the triplet for benzene-d_6 at δ 128.0 (vs TMS) and the central peak of the triplet for chloroform-d_1 at δ 77.0 (vs TMS) were used as internal ^{13}C NMR references. Computer simulations of ^{1}H NMR splitting patterns were performed with SpinWorks, version 2.1.[22]

General Procedures. All syntheses were carried out on a double-manifold, high-vacuum line or in a Vacuum Atmospheres glovebox equipped with an HE-493 Dri-Train. Reactions were typically carried out in pressure-equalizing filter frits equipped with high-vacuum Teflon stopcocks and Solv-seal joints. Nitrogen was purified by passage over reduced BTS catalyst and activated 4A molecular sieves. All glassware was thoroughly oven dried and flame dried under vacuum prior to use. NMR sample tubes were sealed under approximately 500 Torr of nitrogen. Elemental analyses were performed by Complete Analysis Laboratories Inc., E+R Microanalytical Division, Parsippany, NJ 07054.

Preparation of $[(C_5H_4)SiMe_2(N\text{-}t\text{-}Bu)]ZrCl_2$, 1. A 4.30 g sample (11.5 mmol) of freshly sublimed $[(C_5H_4)SiMe_2(N\text{-}t\text{-}Bu)]Zr(NMe_2)_2$ was placed in a 100 mL Solv-seal flask. Toluene (25 mL) and 4.0 mL (31.5 mmol, 37% excess) of $SiMe_3Cl$ were added by vacuum transfer. The stirred solution was heated at 65 °C overnight. After removal of the toluene and the excess of $SiMe_3Cl$, washing of the crude product with pentane left **1** as a white finely divided solid. Yield: 3.70 g (91%). Suitable crystals for structural analysis were grown by cooling a saturated toluene solution. ^{1}H NMR ($CDCl_3$): δ 6.91, 6.44 (t, 2H, C_5H_4, $^3J_{H-H}$ = 2.2 Hz), 1.38 (s, 9H, $NCMe_3$), 0.54 (s, 6H, $SiMe_2$). Gated non-decoupled ^{13}C NMR ($CDCl_3$): δ 122.1, 121.2 (C_5H_4, d, J = 175 Hz), 109.8 (bridgehead, s), 57.7 (N**C**Me_3, s), 32.6 (NC**Me**$_3$, q, J =

(31) The bond distances for the pair of terminal and internal Ti−C distances are 2.204(4); 2.244(4) Å and 2.311(4); 2.320(4) Å, respectively, with ΔTi−C being −0.09 Å. The dihedral angle, α, is 106.1°. The ^{1}H NMR spectrum features two multiplets centered at δ 5.01; 4.01 for the meso protons and two pseudo doublets of doublets centered at δ 3.56; 3.32 for the anti protons of the *cis*-1,4-diphenylbutadiene ligand. Morgan, J. B.; Petersen, J. L, unpublished results.

(32) Gordon, A. J.; Ford, R. A. *The Chemist's Companion*; Wiley-Interscience: New York, 1972; pp 431−436.
(33) Sekutowski, D. G.; Stucky, G. D. *Inorg. Chem.* **1975**, *14*, 2192−2199.
(34) A procedure analogous to that described previously for $(C_5Me_4H)SiMe_2(N(H)\text{-}t\text{-}Bu)$[10] was used to prepare $(C_5Me_4H)SiMe_2(N(H)\text{-}i\text{-}Pr)$.
(35) Diamond, G. M.; Rodewald, S.; Jordan, R. F. *Organometallics* **1995**, *14*, 5−7.

125 Hz), 0.90 ($SiMe_2$, q, $J = 120$ Hz). Anal. Calcd for $C_{11}H_{19}Cl_2NSiZr$: C, 37.17; H, 5.39; N, 3.94. Found: C, 37.27; H, 5.67; N, 4.10.

Preparation of [$(C_9H_6)SiMe_2$(N-*t*-Bu)]$ZrCl_2$, 2. A 1.89 g sample (7.00 mmol) of $Zr(NMe_2)_4$ was combined with 1.73 g (7.00 mmol) of $(C_9H_7)SiMe_2$(N(H)-*t*-Bu) in a 100 mL Solv-seal flask. The neat reaction mixture was heated to 120 °C and stirred for 2 days. A modest purge of N_2 and periodic evacuation of the reaction mixture removed the volatile NMe_2H. The reaction proceeded with formation of 3.0 g of $[(C_9H_6)SiMe_2(N\text{-}t\text{-Bu})]Zr(NMe_2)_2$ as a dark orange oil.[9] The entire product was dissolved in 20 mL of toluene. $SiMe_3Cl$ (2.7 mL, 50% excess) was added by vacuum transfer, and the reaction was stirred for 24 h at 65 °C. The resulting product was washed twice with pentane and then purified by sublimation at 55 °C and 10^{-4} Torr. Yield: 2.34 g (83%). Slow removal of CH_2Cl_2 from a saturated solution provided crystals suitable for X-ray crystallographic analysis. ^{1}H NMR ($CDCl_3$): δ 7.75 (d, 2H, $^3J_{H-H} = 8.5$, aromat CH), 7.36, 7.26 (t, 1H, $^3J_{H-H} = 6.5, 8.5$, aromat CH), 7.09, 6.62 (d, 1H, $^3J_{H-H} = 3.1$, olefin. CH), 1.33 (s, 9H, $NCMe_3$), 0.88, 0.62 (s, 3H, $SiMe_2$). Gated non-decoupled ^{13}C NMR ($CDCl_3$): δ 132.9, 132.8 (s, aromat), 127.7, 127.5, 126.4, 125.6 (d, CH, aromat, $J = 161$ Hz), 126.4, 111.1 (d, CH, olefin., $J = 175$, 169 Hz), 94.0 (s, bridgehead), 57.1 (s, **C**Me_3), 32.7 (q, C**Me**$_3$, $J = 125$ Hz), 3.92, 1.78 (q, $SiMe_2$, $J = 119$ Hz). Anal. Calcd for $C_{15}H_{21}Cl_2NSiZr$: C, 44.43; H, 5.22; N, 3.45. Found: C, 44.37; H, 5.29; N, 3.54.

Preparation of [$(C_5Me_4)SiMe_2$(N-*i*-Pr)]$ZrCl_2$, 3. A 1.00 g sample of freshly sublimed $Zr(NMe_2)_4$ was combined with 0.90 g of $(C_5Me_4H)SiMe_2$(N(H)-*i*-Pr) in a 100 mL Solv-seal flask. The neat reaction mixture was heated to 100 °C while under a modest N_2 flush and *within an hour* a light yellow crystalline product formed. The NMR data indicated that this amine elimination reaction was essentially quantitative. Crude isolated yield: 1.45 g, 93.5%. ^{1}H NMR (C_6D_6): δ 3.81 (septet, 1H, $^3J_{H-H} = 7.1$, C**H**Me_2), 2.88 (s, 12H, NMe_2), 2.15, 1.90 (s, 6H, C_5Me_4), 1.19 (d, 6H, $^3J_{H-H} = 7.1$, CH**Me**$_2$), 0.59 (s, 6H, $SiMe_2$). Gated non-decoupled ^{13}C NMR (C_6D_6): δ 127.6, 124.0 (s, C_5Me_4), 101.1 (s, bridgehead C of C_5Me_4), 50.7 (d, **C**HMe_2, $J = 132$ Hz), 44.1 (q, NMe_2, $J = 131$ Hz), 28.7 (q, CH**Me**$_2$, $J = 126$ Hz), 13.9, 11.0 (q, C_5Me_4, $J = 126$ Hz), 6.1 (q, $SiMe_2$, $J = 118$ Hz).

The 1.45 g sample of $[(C_5Me_4)SiMe_2(N\text{-}i\text{-Pr})]Zr(NMe_2)_2$ was used without further purification and transferred to a 100 mL Solv-seal flask. Toluene (25 mL) and 1.14 g of $SiMe_3Cl$ (50% excess) were added via vacuum transfer. After the reaction mixture was stirred for 2 days at ambient temperature, the volatiles were removed and the product residue was washed with a small amount of pentane. Yield: 1.25 g (90%). The cooling of a saturated toluene solution afforded crystals suitable for X-ray crystallographic analysis. ^{1}H NMR (C_6D_6): δ 4.03 (sept., C**H**Me_2, $^3J_{H-H} = 6.4$), 2.05, 1.94 (s, C_5Me_4), 1.19 (d, CH**Me**$_2$, $^3J_{H-H} = 6.4$), 0.39 (s, $SiMe_2$). ^{13}C{^{1}H} NMR (C_6D_6): δ 134.5, 130.4 (**C**$_5Me_4$), 101.8 (bridgehead C of C_5Me_4), 50.7 (**C**HMe_2), 26.1 (CH**Me**$_2$), 14.9, 11.8 (C_5**Me**$_4$), 4.8 ($SiMe_2$). Anal. Calcd for $C_{14}H_{25}Cl_2NSiZr$: C, 42.30; H, 6.34; N, 3.52. Found: C, 42.35; H, 6.52; N, 3.30.

Preparation of Activated Mg. A 100 mL Solv-seal flask was charged with 6.00 g (0.25 mol) of Mg chips and 0.30 g of iodine. THF (60 mL, dried over Na/K benzophenone ketyl) was added to the reaction flask via vacuum transfer. Approximately 1.0 mL of 2,3-dimethyl-1,3-butadiene was condensed into the reaction flask. The reaction mixture was heated to 65 °C and stirred for 1.5 days. The yellowish-green solution was filtered, leaving gray Mg chips, which were washed with THF (2 × 10 mL).

Preparation of $[Mg(C_4H_4Ph_2)(THF)_3]_n$.[36] A 3.05 g sample of activated Mg and 2.50 g of *trans*-1,4-diphenylbutadiene were added to a 100-mL round-bottom Solv-seal flask. Following evacuation of the filter frit assembly, THF (60 mL, dried over Na/K benzophenone ketyl) was added via vacuum distillation. The flask containing the reaction mixture was placed in a thermostatically controlled water bath to maintain the temperature at 15 °C. The reaction mixture was stirred continuously for 5 days. The filter frit assembly was placed on the vacuum line, and the red solution was filtered, leaving an orange solid and Mg chips. THF was removed into a liquid nitrogen-cooled trap. The THF was redistilled back to extract the remaining product. After the THF was removed under vacuum, the orange pyrophoric product was washed several times with pentane. Yield: 4.70 g (89%)

Preparation of [$(C_5H_4)SiMe_2$(N-*t*-Bu)]$Zr(C_4H_4Ph_2)$, 4. A 0.50 g (1.41 mmol) sample of $[(C_5H_4)SiMe_2(N\text{-}t\text{-Bu})]ZrCl_2$ and 0.64 g (1.48 mmol, 5% excess) of $[Mg(C_4H_4Ph_2)(THF)_3]_n$ were combined in a 100 mL Solv-seal flask that was then attached to a swivel frit assembly. Toluene (30 mL) was added via vacuum distillation. After the reaction mixture was stirred for 3 h at room temperature, the solution was filtered. The solvent was removed slowly into a liquid nitrogen-cooled trap, leaving dark red crystals. The product was recrystallized from toluene. Yield: 0.55 g (80%). Anal. Calcd for $C_{30.5}H_{37}SiZrN$ (536.92): C, 68.23; H, 6.95; N, 2.60. Found: C, 68.01; H, 6.75; N, 2.65. Major isomer, ^{1}H NMR (599.67 MHz, C_6D_6): δ 7.23 (mult., $4H_m$, meta Ph), 7.05 (mult., $4H_o$, ortho Ph), 6.92 (tt, $2H_p$, para Ph), 6.28 (mult., $2H_{meso}$, meso butadiene), 5.95 (t, 2H, C_5H_4, $^3J_{H-H} = 2.3$), 5.74 (t, 2H, C_5H_4, $^3J_{H-H} = 2.3$), 1.97 (mult., $2H_{anti}$, anti butadiene), 0.98 (s, 9H, CMe_3), 0.20 (s, 6H, $SiMe_2$). Proton coupling constants (Hz) determined by computer simulation of the phenyl protons: $J_{m-m'} = 1.05(6)$, $J_{m-p} = 7.30(5)$, $J_{m-o} = 7.13(8)$, $J_{o-m'} = 1.21(1)$, $J_{p-o} = 1.15(5)$, $J_{o-o'} = 0.32(6)$. Proton coupling constants (Hz) determined by computer simulation of the butadiene protons: $J_{meso-meso'} = 9.94(6)$, $J_{meso-anti'} = -2.12(8)$, $J_{anti-anti'} = 0.22(5)$, $J_{anti-meso} = 11.18(1)$. Gated non-decoupled ^{13}C NMR (67.5 MHz, C_6D_6): δ 143.1 (s, ipso Ph), 129.3 (d, meta Ph, $J = 153$), 122.5 (d, para Ph, $J = 154$), 121.6 (d, ortho Ph, $J = 153$), 120.1 (d, meso butadiene, $J = 158$), 116.8 (d, C_5H_4, $J = 162$), 116.3 (d, C_5H_4, $J = 170$), 110.8 (s, bridgehead), 75.0 (d, anti butadiene, $J = 138$), 59.4 (s, **C**Me_3), 36.1 (q, C**Me**$_3$, $J = 123$), 2.2 (q, $SiMe_2$, $J = 118$). 2D HETCOR (C_6D_6): δ 129.3/7.23 (meta Ph), 122.5/6.92 (para Ph), 121.6/7.05 (ortho Ph), 120.1/6.28 (meso butadiene), 116.8/5.95 (C_5H_4), 116.3/5.74 (C_5H_4), 75.0/1.97 (anti butadiene), 36.1/0.98 (C**Me**$_3$), 2.2/0.20 ($SiMe_2$). Minor isomer, ^{1}H NMR (599.67 MHz, C_6D_6): δ 7.3−6.9 (Ph), 5.86 (t, 2H, C_5H_4, $^3J_{H-H} = 2.5$), 5.47 (t, 2H, C_5H_4, $^3J_{H-H} = 2.5$), 5.12 (mult., $2H_{meso}$, meso butadiene), 2.70 (mult., $2H_{anti}$, anti butadiene), 1.10 (s, 9H, CMe_3), 0.31 (s, 6H, $SiMe_2$). Proton coupling constants (Hz) determined by computer simulation for the butadiene protons: $J_{meso-meso'} = 11.44(7)$, $J_{meso-anti'} = -1.76(10)$, $J_{anti-anti'} = 0.29(6)$, $J_{anti-meso} = 12.59(1)$.

Preparation of [$(C_9H_6)SiMe_2$(N-*t*-Bu)]$Zr(C_4H_4Ph_2)$, 5. A 0.50 g (1.23 mmol) sample of $[(C_9H_6)SiMe_2(N\text{-}t\text{-Bu})]ZrCl_2$ and 0.56 g (1.29 mmol, 5% excess) of $[Mg(C_4H_4Ph_2)(THF)_3]_n$ were added to a 100 mL Solv-seal flask. The reaction mixture was stirred in 30 mL of toluene for 3 h at room temperature and then filtered through a filter frit. While the solvent was removed slowly, crystals formed on the wall of the flask. Larger dark red crystals were obtained by recrystallization with pentane. Yield: 0.43 g (64%). Anal. Calcd for $C_{34.5}H_{39}SiZrN$ (586.98): C, 70.59; H, 6.70; N, 2.39. Found: C, 70.31; H, 6.85; N, 2.28.

(36) Yasuda, H.; Kajihara, Y.; Mashima, K.; Nagasuna, K.; Lee, K.; Nakamura, A. *Organometallics* **1982**, *1*, 388−396.

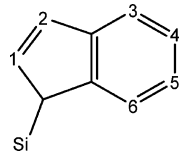

Major isomer, ^{1}H NMR (599.67 MHz, C_6D_6): δ 7.28 (mult., $2H_m$, Ph_1), 7.06 (mult., $2H_o$, Ph_1), 6.93 (tt, H_p, Ph_1), 7.16 (mult., $2H_m$, Ph_2), 6.98 (tt, H_p, Ph_2), 6.56 (mult., $2H_o$, Ph_2), 7.57, 7.09, 6.84, 6.51, 6.32, 5.71 (dq, dt, ddd, ddd, d, dd; H_3, H_6, H_4, H_5, H_1, H_2; $J_{1,2} = 3.3$, $J_{2,3} = 0.9$, $J_{3,4} = 8.4$, $J_{3,5} = 1.2$, $J_{3,6} = 1.0$, $J_{4,5} = 6.6$, $J_{4,6} = 1.2$, $J_{5,6} = 8.5$ Hz), 6.15, 6.11 (mult., 2H, meso butadiene), 1.72, 1.25 (mult., 2H, anti butadiene), 0.92 (s, 9H, CMe_3), 0.65, 0.20 (s, 6H, $SiMe_2$); proton coupling constants (Hz) determined by computer simulation for Ph_1: $J_{m-m'} = 0.93(8)$, $J_{m-p} = 7.31(6)$, $J_{m-o} = 7.21(9)$, $J_{o-m'} = 0.96(1)$, $J_{p-o} = 1.28(6)$, $J_{o-o'} = 0.34(8)$. Proton coupling constants (Hz) determined by computer simulation for Ph_2: $J_{m-m'} = 0.9(1)$, $J_{m-p} = 7.1(1)$, $J_{m-o} = 7.0(2)$, $J_{o-m'} = 0.86(2)$, $J_{p-o} = 1.3(1)$, $J_{o-o'} = 0.3(1)$. Proton coupling constants (Hz) determined by computer simulation of the butadiene protons: $J_{meso1-meso2} = 10.70(7)$, $J_{meso1-anti1} = 11.84(7)$, $J_{meso2-anti1} = 1.17(7)$, $J_{meso1-anti2} = 1.34(7)$, $J_{meso2-anti2} = 12.03(7)$, $J_{anti1-anti2} = 0.16(7)$. ^{13}C{^{1}H} NMR (67.5 MHz, C_6D_6): δ 143.9, 142.5 (ipso-Ph), 133.2, 129.6 (quat. C, indenyl), 125.1, 124.6, 124.5, 124.2, 121.7, 107.0 (C_6, C_3, C_5, C_4, C_1, C_2), 128.8, 123.2, 122.9 ($2C_m$, $2C_o$, C_p of Ph_1), 127.4, 125.3, 122.7 ($2C_m$, $2C_o$, C_p of Ph_2), 122.6, 117.5 (meso butadiene), 96.5 (bridgehead C, indenyl), 79.6, 77.1 (anti butadiene), 59.1 (**C**Me_3), 35.8 (C**Me**$_3$), 6.3, 2.2 ($SiMe_2$). 2D HETCOR (C_6D_6): δ 125.1/7.09, 124.6/7.57, 124.5/6.84, 124.2/6.51, 121.7/6.32, 107.0/5.71 (CH, indenyl), 128.8/7.28, 123.2/7.06, 122.9/6.93 (CH, Ph_1), 127.4/7.16, 125.3/6.56, 122.7/6.98 (CH, Ph_2), 122.6/6.11, 117.5/6.15 (CH, meso butadiene), 79.6/1.72, 77.1/1.25 (CH, anti butadiene), 35.8/0.92 (CMe_3), 6.3/0.65, 2.2/0.20 ($SiMe_2$). Minor isomer, ^{1}H NMR (599.67 MHz, C_6D_6): δ 7.5−6.4 (mult., 16H, Ph and indenyl rings), 5.31, 4.42 (mult., 2H, meso butadiene), 2.58, 2.43 (mult., 2H, anti butadiene), 1.10 (s, 9H, CMe_3), 0.69, 0.40 (s, 6H, $SiMe_2$). Proton coupling constants (Hz) determined by computer simulation of the butadiene protons: $J_{meso1-meso2} = 11.5(2)$, $J_{meso1-anti1} = 12.3(2)$, $J_{meso2-anti1} = 1.3(2)$, $J_{meso1-anti2} = 1.6(2)$, $J_{meso2-anti2} = 12.5(2)$, $J_{anti1-anti2} = 0.2(2)$.

Preparation of [(C_5Me_4)$SiMe_2$(N-*i*-Pr)]Zr($C_4H_4Ph_2$), 6. A 20 mL cylindrical Solv-seal tube was charged with 0.10 g (0.25 mmol) of [(C_5Me_4)$SiMe_2$(N-*i*-Pr)]$ZrCl_2$ and 0.12 g (0.26 mmol, 5% excess) of $[Mg(C_4H_4Ph_2)(THF)_3]_n$. The reaction mixture was stirred in 15 mL of toluene for 1 h at 0 °C before being warmed to room temperature and then stirred for an additional hour. The reaction mixture was filtered, and the solvent was removed slowly under reduced pressure, leaving the product as dark red crystals. Yield: 0.12 g (88%) Anal. Calcd for $C_{30}H_{39}SiZrN$ (532.93): C, 67.61; H, 7.38; N, 2.63. Found: C, 67.47; H, 7.47; N, 2.56. ^{1}H NMR (599.67 MHz, C_6D_6): δ 7.22 (mult., $4H_m$, meta Ph), 6.94 (tt, $2H_p$, para Ph), 6.89 (mult., $2H_o$, ortho Ph), 6.22 (mult., 2H, meso butadiene), 4.14 (sept., 1H, C**H**Me_2, $^3J_{H-H} = 6.4$), 1.70 (mult., 2H, anti butadiene), 1.67 (s, 12H, C_5**Me**$_4$), 0.96 (d, 6H, CH**Me**$_2$, $^3J_{H-H} = 6.4$), 0.41 (s, 6H, $SiMe_2$). Proton coupling constants (Hz) determined by computer simulation of the phenyl protons: $J_{m-m'} = 1.04(7)$, $J_{m-p} = 7.24(5)$, $J_{m-o} = 7.00(8)$, $J_{o-m'} = 1.19(1)$, $J_{p-o} = 1.17(5)$, $J_{o-o'} = 0.31(7)$. Proton coupling constants (Hz) determined by computer simulation of the butadiene protons: $J_{meso-meso'} = 10.77(5)$, $J_{meso-anti'} = -2.26(7)$, $J_{anti-anti'} = 0.60(4)$, $J_{anti-meso} = 10.96(1)$. Gated non-decoupled ^{13}C NMR (67.5 MHz, C_6D_6): δ 145.0 (s, ipso Ph), 128.6 (d, meta Ph, $J = 154$), 124.1 (d, meso butadiene, $J = 154$), 123.6 (d, ortho Ph, $J = 152$), 122.4 (d, para Ph, $J = 167$), obscured, 124.4 (proximal and distal C_5Me_4), 101.4 (s, bridgehead), 75.4 (d, anti butadiene, $J = 137$), 53.5 (d, **C**HMe_2, $J = 125$), 28.8 (q, CH**Me**$_2$, $J = 125$), 12.8, 10.7 (q, C_5**Me**$_4$, $J = 125$), 6.8 (q, $SiMe_2$, $J = 119$). 2D HETCOR (C_6D_6): δ 128.6/7.22 (meta Ph), 124.1/6.22 (meso butadiene), 122.4/6.94 (para Ph), 123.6/6.89 (ortho Ph), 75.4/1.70 (anti butadiene), 53.5/4.14 (**C**HMe_2), 28.8/0.96 (CH**Me**$_2$), 12.8, 10.7/1.67 (C_5**Me**$_4$), 6.8/0.41 ($SiMe_2$).

Preparation of [(C_5Me_4)$SiMe_2$(N-*t*-Bu)]Zr($C_4H_4Ph_2$), 7. A 100 mL Solv-seal flask was charged with 0.50 g (1.22 mmol) of [(C_5Me_4)$SiMe_2$(N-*t*-Bu)]$ZrCl_2$ and 0.56 g (1.28 mmol, 5% excess) of $[Mg(C_4H_4Ph_2)(THF)_3]_n$. Following the addition of 30 mL of toluene, the reaction mixture was stirred for 3 h at room temperature. The resulting reaction mixture was filtered, and the solvent was removed slowly into a liquid nitrogen-cooled trap. The dark reddish-brown product contained a mixture of two isomers. After the solid was washed with pentane, the major isomer was recrystallized from toluene. Yield: 0.63 g (94%). Major isomer, ^{1}H NMR (599.67 MHz, C_6D_6): δ 7.22 (mult., $4H_m$, meta Ph), 7.00 (mult., $4H_o$, ortho Ph), 6.96 (tt, $2H_p$, para Ph), 6.38 (mult., meso butadiene), 1.78 (s, 6H, C_5Me_4), 1.64 (s, 6H, C_5Me_4), 1.37 (mult., anti butadiene), 1.14 (s, 9H, CMe_3), 0.48 (s, 6H, $SiMe_2$). Proton coupling constants (Hz) determined by computer simulation of the phenyl protons: $J_{m-m'} = 1.13(15)$, $J_{m-p} = 7.01(11)$, $J_{m-o} = 6.50(18)$, $J_{o-m'} = 1.21(3)$, $J_{p-o} = 1.17(11)$, $J_{o-o'} = 0.29(11)$. Proton coupling constants (Hz) determined by computer simulation of the butadiene protons: $J_{meso-meso'} = 10.55(7)$, $J_{meso-anti'} = -2.2(1)$, $J_{anti-anti'} = 0.43(6)$, $J_{anti-meso} = 11.28(1)$. ^{13}C{^{1}H} NMR (67.5 MHz, C_6D_6): δ 145.4 (ipso Ph), 128.4 (meta Ph), 124.8 (ortho Ph), 124.0 (meso butadiene), 122.8 (para Ph), 125.6, 125.3 (proximal and distal **C**$_5$-Me_4), 103.3 (bridgehead **C**$_5Me_4$), 76.3 (anti butadiene), 55.8 (**C**Me_3), 36.5 (C**Me**$_3$), 13.1, 11.2 (C_5**Me**$_4$), 7.8 ($SiMe_2$). 2D HETCOR (C_6D_6): δ 128.4/7.22 (meta Ph), 124.8/7.00 (ortho Ph), 122.8/6.96 (para Ph), 124.0/6.38 (meso butadiene), 76.3/1.37 (anti butadiene), 36.5/1.14 (C**Me**$_3$), 13.1/1.78 (C_5**Me**$_4$), 11.2/1.64 (C_5**Me**$_4$), 7.8/0.48 ($SiMe_2$). Minor isomer, ^{1}H NMR (599.67 MHz, C_6D_6): δ 7.3−7.1 (mult., 10H, Ph), 5.01 (mult., meso butadiene), 2.83 (mult., anti butadiene), 1.75 (s, 6H, C_5Me_4), 1.37 (s, 6H, C_5Me_4), 1.21 (s, 9H, CMe_3), 0.56 (s, 6H, $SiMe_2$). Proton coupling constants (Hz) determined by computer simulation of the butadiene protons: $J_{meso-meso'} = 11.41(9)$, $J_{meso-anti'} = -1.5(1)$, $J_{anti-anti'} = 0.24(7)$, $J_{anti-meso} = 13.05(3)$. ^{13}C{^{1}H} NMR (67.5 MHz, C_6D_6): δ 144.2 (ipso Ph), 128.7, 126.8, 124.0 (Ph), 129.8, 124.3 (proximal and distal **C**$_5Me_4$), 105.1 (meso butadiene), 99.2 (bridgehead), 77.7 (anti butadiene), 55.6 (**C**Me_3), 36.3 (C**Me**$_3$), 13.2, 11.0 (C_5**Me**$_4$), 7.9 ($SiMe_2$). 2D HETCOR (C_6D_6): δ 128.7/7.14, 126.8/7.30, 124.0/7.25 (Ph); 105.1/5.01 (meso butadiene), 77.7/2.83 (anti butadiene), 36.3/1.21 (C**Me**$_3$), 13.2/1.75 (C_5**Me**$_4$), 11.0/1.37 (C_5**Me**$_4$), 7.9/0.56 ($SiMe_2$).

Description of the X-ray Structural Analyses. The crystals for **1**−**3** were sealed in glass capillary tubes under a nitrogen atmosphere. The data collections for {[(C_5H_4)$SiMe_2$(N-*t*-Bu)]ZrCl-(μ-Cl)}$_2$ and [(C_9H_6)$SiMe_2$(N-*t*-Bu)]$ZrCl_2$ were performed at ambient temperature, whereas that of {[(C_5Me_4)$SiMe_2$(N-*i*-Pr)]ZrCl(μ-Cl)}$_2$ was carried out while cooling the sample at −80 °C, with a stream of nitrogen gas provided by an LT-2 low-temperature attachment. The reflections that were used for the unit-cell determination were located and indexed by the automatic peak search routine provided with XSCANS.[37] The lattice parameters and orientation matrix for the unit cells were calculated from a nonlinear least-squares fit of the orientation angles of at least 35 reflections. The X-ray diffraction data for [(C_9H_6)$SiMe_2$(N-*t*-Bu)]-

(37) XSCANS (version 2.0) is a diffractometer control system developed by Bruker AXS, Inc., Madison, WI.

$ZrCl_2$ were initially collected using an I-centered monoclinic unit cell and later transformed to the conventional C-centered monoclinic cell.

Intensity data were measured with graphite-monochromated Mo Kα radiation ($\lambda = 0.71073$ Å) and variable ω scans. Background counts were measured at the beginning and at the end of each scan with the crystal and counter kept stationary. The combined intensities of three standard reflections, which were measured after every 100 reflections, did not show any indication of crystal movement or decay. The raw data were corrected for Lorentz-polarization effects. An empirical absorption correction based on the measurement of six PSI scans was applied to the data collected for $\{[(C_5H_4)SiMe_2(N\text{-}t\text{-}Bu)]ZrCl(\mu\text{-}Cl)\}_2$.

The crystals of **4**−**7** were coated with the perfluoropolyether PFO-XR75 (Lancaster) and then sealed under nitrogen in glass capillary tubes. Each sample was optically aligned on the four-circle of a Siemens P4 diffractometer equipped with a graphite monochromatic crystal, a Mo Kα radiation source ($\lambda = 0.71073$ Å), and a SMART CCD detector held at 5.054 cm from the crystal. The samples were cooled to −50 °C. Four sets of 20 frames each were collected using the ω scan method, with a 10 s exposure time. Integration of these frames followed by reflection indexing and least-squares refinement produced a crystal orientation matrix and preliminary lattice parameters.

Data collection involved the measurement of a total of 1650 frames of 30 s duration in five different runs covering a hemisphere. The program SMART (version 5.6)[38] was used for diffractometer control, frame scans, indexing, orientation matrix calculations, least-squares refinement of cell parameters, and data collection. All of the raw data frames were read by the program SAINT (version 5/6.0)[38] and integrated using 3D profiling algorithms. An absorption correction was applied using the SADABS routine available in SAINT. The data were corrected for Lorentz and polarization effects, as well as any crystal decay.

Initial coordinates for all of the non-hydrogen atoms were determined by a combination of direct methods and difference Fourier methods with the use of SHELXL-93 or SHELXTL 6.1.[39] The molecular structures of $\{[(C_5H_4)SiMe_2(N\text{-}t\text{-}Bu)]ZrCl(\mu\text{-}Cl)\}_2$ and $\{[(C_5Me_4)SiMe_2(N\text{-}i\text{-}Pr)]ZrCl(\mu\text{-}Cl)\}_2$ are constrained in the solid state by a crystallographic center of inversion. The structural analyses of $[(C_5Me_4)SiMe_2(N\text{-}t\text{-}Bu)]Zr(C_4H_4Ph_2)$ and $[(C_5H_4)SiMe_2(N\text{-}t\text{-}Bu)]Zr(C_4H_4Ph_2)$ revealed the presence of toluene, which was disordered about a crystallographic center of inversion. The three methyls of the *tert*-butyl substituent bound to the amido N in $[(C_5Me_4)SiMe_2(N\text{-}t\text{-}Bu)]Zr(C_4H_4Ph_2)$ suffered from a two-site 75:25 disorder. Idealized positions for the hydrogen atoms were included as fixed contributions using a riding model, and the positions of the methyl hydrogen atoms were optimized by a rigid rotating group refinement with idealized tetrahedral angles. Full-matrix least-squares refinement based upon the minimization of $\sum w_i |F_o^2 - F_c^2|^2$, with weighting given by the expression $w_i^{-1} = [\sigma^2(F_o^2) + (aP)^2 + bP]$, where $P = (\mathrm{Max}(F_o^2,0) + 2F_c^2)/3$, converged to give the values of the final discrepancy indices[40] provided in Table 2. Selected interatomic distances and bond angles are summarized in Tables 3 and 4 for the Zr dichloride complexes **1**−**3** and the Zr 1,4-diphenylbutadiene derivatives **4**−**7**, respectively.

Acknowledgment. Financial support for this research was provided by the donors of the Petroleum Research Fund, administered by the American Chemical Society. J.L.P. gratefully acknowledges the financial support provided by the Eberly College of Arts and Sciences and the C. Eugene Bennett Department of Chemistry and the unrestricted research funds provided by Union Carbide Corp. and The Dow Chemical Co. to acquire a SMART CCD detector for the Siemens P4 X-ray diffractometer at West Virginia University. Funds for the recent acquisition of a Varian 600 Inova NMR spectrometer at West Virginia University were provided through the NSF-EPsCOR program.

Note Added after ASAP: The version of this paper posted ASAP May 27, 2004, was missing the Results and Discussion section heading. The corrected version appeared June 7, 2004.

Supporting Information Available: Complete tables of the results from the X-ray crystallographic analyses performed on compounds **1**−**7**. This material is available free of charge via the Internet at http://pubs.acs.org.

IC040001I

(38) The SMART 5.6 and SAINT 5/6.0 programs are part of the Bruker AXS crystallographic software package used for single-crystal data collection, reduction, and preparation.

(39) SHELXTL-93 and SHELXTL 6.1 are crystallographic software packages developed by Professor G. Sheldrick, Institut fur Anorganische Chemie, University of Göttingen, D-37077 Göttingen, Germany, for Bruker AXS, Inc., Madison, WI.

(40) The equations for the R-factors are $R1 = \sum(||F_o| - |F_c||)/\sum|F_o|$ and $wR2 = [\sum[w(F_o^2 - F_c^2)^2]/\sum[wF_o^2]]^{1/2}$. The expression for the "goodness-of-fit" is $GOF = [\sum[w(F_o^2 - F_c^2)^2]/(n-p)]^{1/2}$, where n is the number of reflections and p is the total number of parameters that were varied during the last refinement cycle.